

# HEMGS: A Hybrid Entropy Model for 3D Gaussian Splatting Data Compression

Lei Liu  
Beihang University  
Beijing, China

liulei95@buaa.edu.cn

Zhenhao Chen  
The University of Newcastle  
Newcastle, Australia

zhenghao.chen@newcastle.edu.au

Dong Xu\*  
The University of HongKong  
Hong Kong SAR, China

dongxu@cs.hku.hk

## Abstract

*Fast progress in 3D Gaussian Splatting (3DGS) has made 3D Gaussians popular for 3D modeling and image rendering, but this creates big challenges in data storage and transmission. To obtain a highly compact 3DGS representation, we propose a hybrid entropy model for Gaussian Splatting (HEMGS) data compression, which comprises two primary components, a hyperprior network and an autoregressive network. To effectively reduce structural redundancy across attributes, we apply a progressive coding algorithm to generate hyperprior features, in which we use previously compressed attributes and location as prior information. In particular, to better extract the location features from these compressed attributes, we adopt a domain-aware and instance-aware architecture to respectively capture domain-aware structural relations without additional storage costs and reveal scene-specific features through MLPs. Additionally, to reduce redundancy within each attribute, we leverage relationships between neighboring compressed elements within the attributes through an autoregressive network. Given its unique structure, we propose an adaptive context coding algorithm with flexible receptive fields to effectively capture adjacent compressed elements. Overall, we integrate our HEMGS into an end-to-end optimized 3DGS compression framework and the extensive experimental results on four benchmarks indicate that our method achieves about 40% average reduction in size while maintaining the rendering quality over our baseline method and achieving state-of-the-art compression results.*

## 1. Introduction

In the past few years, considerable progress has been achieved in the field of novel view synthesis for 3D scene representation. Neural Radiance Field (NeRF) [27] represents 3D scenes as continuous radiance fields, which learns the geometric shape and appearance information of

the scene through an implicit Multilayer Perceptron (MLP), thus it can render high-definition images of the scene from new viewpoints. Although NeRF yields effective results, the slow rendering speed has, to some extent, limited its development. Recently, 3D Gaussian Splatting (3DGS) [17] has emerged as a novel paradigm in 3D scene representation, which introduces learnable Gaussians to explicitly model 3D scenes. Due to its rapid training and rendering capabilities, 3DGS has been widely applied for novel view synthesis.

However, 3DGS requires substantial 3D Gaussians and associated attributes for effectively rendering scenes, which will bring significant challenges for storage during deployment. Therefore, it is emergent to develop effective 3DGS data compression methods. Some early works intuitively reduce the number of parameters by using the vector quantization strategy to cluster the Gaussian parameters and store them into a predefined codebook [9, 20, 30, 31] or directly pruning parameters [9, 20]. Though, such methods intuitively achieve data compression without adequately exploiting the structural redundancies in 3DGS, which limits the compression performance.

To achieve better compression performance, recent methods [3, 26, 29] have explored the structural relations in 3DGS. For instance, Lu *et al.* proposed ScaffoldGS [26], which uses anchors to capture such relations of 3D Gaussians. Chen *et al.* adopted a Hash-grid Assisted Context (HAC) [3] strategy to further acquire continuous spatial consistency among anchors using the binary hash grid structure. While the methods mentioned above intuitively exploit structural redundancy through the effective data structure, there is still significant potential to further improve compression efficiency. In most compression tasks, a powerful entropy model is among the most effective tools for uncovering various relationships within the data [1, 8, 16, 21, 25, 28], which is crucial for efficient encoding and storage reduction. However, the potential of entropy models within the 3DGS data structure is largely unexplored.

In this work, we propose a hybrid entropy model for

\*Dong Xu is the corresponding author.

Gaussian Splatting (HEMGS) data to effectively capture structural redundancies and reduce storage requirements for 3DGS data. Our work is inspired by the remarkable success of joint entropy models in neural image (NIC) [1, 8, 28] and video compression (NVC) [16, 21, 25]. Building on Scaffold-GS [26], our HEMGS exploits relationships across anchor attributes and within each attribute by utilizing a hyperprior network and an autoregressive network, respectively.

First, to better leverage structural relationships across attributes, we employ a progressive coding algorithm to generate hyperprior features through a hyperprior network. This method first encodes location and certain attributes, and then utilizes the extracted features from this compressed information as priors to perform conditional entropy coding for subsequent attributes. Specifically, we begin by compressing the anchor location, which provides critical information for encoding other attributes (*e.g.*, local features), then we subsequently compress scaling and offsets. Extracting location features, however, is a challenging task, as most existing methods [3, 26] primarily store instance-aware structural relations in MLPs. In contrast, we integrate both domain-aware and instance-aware architectures, in which we utilize a pre-trained 3D feature extraction network (*i.e.*, PointNet++ [33]) as our Domain-Aware Network to capture domain-aware structural relations without incurring additional storage costs. By combining the captured domain-aware and instance-aware structural relations, where the Instance-Aware Network (*i.e.*, hash grid [3]) encodes instance-aware information, we create a comprehensive hyperprior. This enables more accurate distribution estimation for anchor attributes, leading to enhanced conditional entropy coding efficiency.

Additionally, to exploit structural redundancy within each attribute, we integrate an autoregressive network into our 3DGS compression approach. Inspired by the foundational works in NIC research [8, 13, 28, 34, 35], we generate context features from previously compressed elements within the anchor attribute to improve probability estimation. Given the unique structure of 3DGS, which is characterized by its unordered nature and varying anchor densities across regions, we propose an adaptive context coding algorithm with flexible receptive fields to capture compressed elements effectively. Specifically, for sparse areas, we employ a larger receptive field to gather a broader context, while for denser regions, we limit the context to the nearest  $n$  elements to focus on adjacent elements relevant to the coding element. This approach allows us to better capture contextual relevance, thereby reducing redundancy within each attribute more effectively.

Overall, we integrate our HEMGS with several other coding components (*e.g.*, adaptive quantization) into an end-to-end optimized 3DGS data compression framework,

which efficiently reduces the redundancy within and across anchor attributes and achieves start-of-the-art 3DGS data compression performance. Extensive experiments are conducted on various 3DGS data compression benchmarks, including DeepBlending [14], Tank&Temples [19], Mip-NeRF360 [2], and Synthetic-NeRF [27], to demonstrate the superiority of our compression framework. The results demonstrate that our newly-proposed compression method achieves the start-of-the-art compression performance, which achieves about 40% average reduction in size over our baseline method while maintaining high rendering quality. Our contributions can be summarized below:

- We introduce a hyperprior network in combination with a progressive coding algorithm to exploit structural redundancies across attributes, which can generate hyperprior features based on previously-compressed attributes and anchor location. To effectively fuse location features, our hyperprior network adopts a domain-aware and instance-aware network architecture.
- We propose an autoregressive network to exploit structural redundancies within attributes. An adaptive context coding algorithm captures adjacent compressed elements to produce context features for encoding each element, whose receptive fields are adjusted to sparsity levels to ensure efficient coding.
- By combining a hyperprior and an autoregressive network, we introduce an entropy model HEMGS, which can effectively exploit structural redundancy both across and within each attribute. With other coding components, our HEMGS is seamlessly integrated to an end-to-end optimized 3DGS data compression network, achieving a highly compact representation.
- Extensive experimental results validate the effectiveness of our 3DGS data compression framework with our newly proposed HEMGS, which shows state-of-the-art performance across various 3DGS compression benchmarks. Particularly it saves about 40% average storage while maintaining the rendering performance than our baseline.

## 2. Related Work

### 2.1. 3D Gaussian Splatting Data Compression

3D Gaussian Splatting (3DGS) represents 3D scenes using learnable shape and appearance attributes encoded as 3D Gaussian distributions. This method provides high-fidelity scene representation while enabling fast training and rendering, which has driven its widespread adoption. However, the large number of Gaussian points and their attributes present significant storage challenges, necessitating the development of effective 3DGS compression techniques.

Early compression methods focused on refining Gaussian parameter values to reduce model complexity. Approaches such as vector quantization grouped parameters

into a pre-defined codebook [9, 20, 30, 31], while other techniques achieved compression by directly pruning parameters [9, 20]. Recent research [3, 26, 29, 36] has investigated structural relationships to improve compression efficiency. For instance, Scaffold-GS [26] introduced anchor-centered features to reduce the number of 3DGS parameters. Building on Scaffold-GS, HAC [3] employs a hash-grid to capture spatial relationships, while ContextGS [36] integrates anchor-level contextual information to capture structural dependencies in 3DGS.

While these methods intuitively achieve 3DGS compression, the core of effective data compression lies in the entropy model. A well-designed entropy model can uncover structural relationships in the data, enabling efficient coding and reducing storage requirements. However, current 3DGS compression methods still have room for improvement in entropy model design. Drawing inspiration from the success of entropy models in NIC methods [1, 8, 28] and NVC methods [16, 21, 25], we propose a hybrid entropy model for 3D Gaussian Splatting (HEMGS). This model combines a hyperprior network to capture redundancies across attributes and an autoregressive network for redundancies within each attribute. Through the combination of these two methods, HEMGS effectively reduces redundancies, leading to highly efficient 3DGS compression.

## 2.2. Neural Entropy Model

Entropy models are widely used in NIC and NVC to predict probability distributions efficiently for images or videos. For example, Minnen *et al.* proposed an image compression method [28] that uses an entropy model combining a hyperprior network and an autoregressive network to capture spatial redundancies in images, achieving notable compression performance. Similar strategies have been applied to other compression [4–8, 12, 13, 15, 16, 21–25, 34, 35] methods, highlighting the crucial role of entropy models in data compression.

Despite their effectiveness, entropy models in NIC and NVC are not directly applicable to 3DGS compression. A key challenge is that 3DGS contains multiple attributes, making it difficult for conventional entropy models to capture spatial redundancies across attributes. Additionally, the sparsity of anchor points in 3DGS limits the effectiveness of autoregressive networks used in NIC and NVC, as their receptive fields are insufficient for capturing meaningful information from sparse data. To address these challenges, we propose a progressive coding algorithm within the hyperprior network. This method uses location features and previously compressed elements as priors to predict uncompressed attributes, effectively reducing redundancies across attributes. Additionally, our autoregressive model employs an adaptive context coding algorithm that adjusts the receptive field size according to the density of anchor points,

enabling it to capture comprehensive and relevant context. These innovations enhance the overall efficiency of 3DGS compression.

## 3. Methodology

### 3.1. Preliminaries

**3D Gaussian Splatting (3DGS)** [17] adopts a collection of Gaussians to represent 3D scenes, with each Gaussian initialized using Structure-from-Motion (SfM) and characterized by a 3D covariance matrix  $\Sigma$  and location  $\mu$ :

$$G(\mathbf{x}) = e^{-\frac{1}{2}(\mathbf{x}-\mu)^T \Sigma^{-1}(\mathbf{x}-\mu)}, \quad (1)$$

where  $\mathbf{x}$  denotes the coordinates of a 3D point. The covariance matrix  $\Sigma$  is expressed as  $\Sigma = \mathbf{R}\mathbf{S}\mathbf{S}^T\mathbf{R}^T$ , where  $\mathbf{R}$  and  $\mathbf{S}$  represent the rotation and scaling matrices, respectively. Each Gaussian is also associated with opacity  $\alpha$  and view-dependent color  $\mathbf{c}$ , which is modeled using Spherical Harmonics[38]. To render an image, the 3D Gaussians are splatted to 2D, and the pixel values are computed using  $\alpha$  and  $\mathbf{c}$ .

**Anchor** structure is introduced by Scaffold-GS [26] to optimize storage requirements. It employs anchors to group Gaussians and infers their attributes from the attributes of these anchors using MLPs. Each anchor is characterized by a position  $\mathbf{x}^a \in \mathbb{R}^3$  and a set of attributes  $\mathcal{A} = \{\mathbf{f}^a \in \mathbb{R}^{D^a}, \mathbf{l} \in \mathbb{R}^6, \mathbf{o} \in \mathbb{R}^{3K}\}$ , where  $\mathbf{f}^a$  represents the anchor’s local feature,  $\mathbf{l}$  represents the scaling factor, and  $\mathbf{o}$  represents the offsets. During the rendering process, the anchor feature  $\mathbf{f}^a$  is fed into the MLPs to produce the attributes for the Gaussians, whose positions are computed by combining  $\mathbf{x}^a$  with  $\mathbf{o}$ , and  $\mathbf{l}$  is used to regulate the positioning and shape of the Gaussians.

### 3.2. HEMGS for 3DGS Data Compression

A powerful entropy model is one of the most effective methods for exploiting complex relationships within data. It is widely recognized as an efficient compression mechanism. However, entropy models for 3DGS remain much less explored in previous work. Here, we propose HEMGS, which consists of two core components: a hyperprior network and an autoregressive network.

#### 3.2.1. Hyperprior Network

To reduce structural redundancies across attributes, we introduce a hyperprior network with a progressive coding algorithm. This network integrates domain-aware and instance-aware networks to better capture redundancies and generate better hyperprior features, as shown in Figure 1.

**Progressive Coding Algorithm.** As an alternative representation in 3DGS, the anchor contains both location information and various attributes including local features,

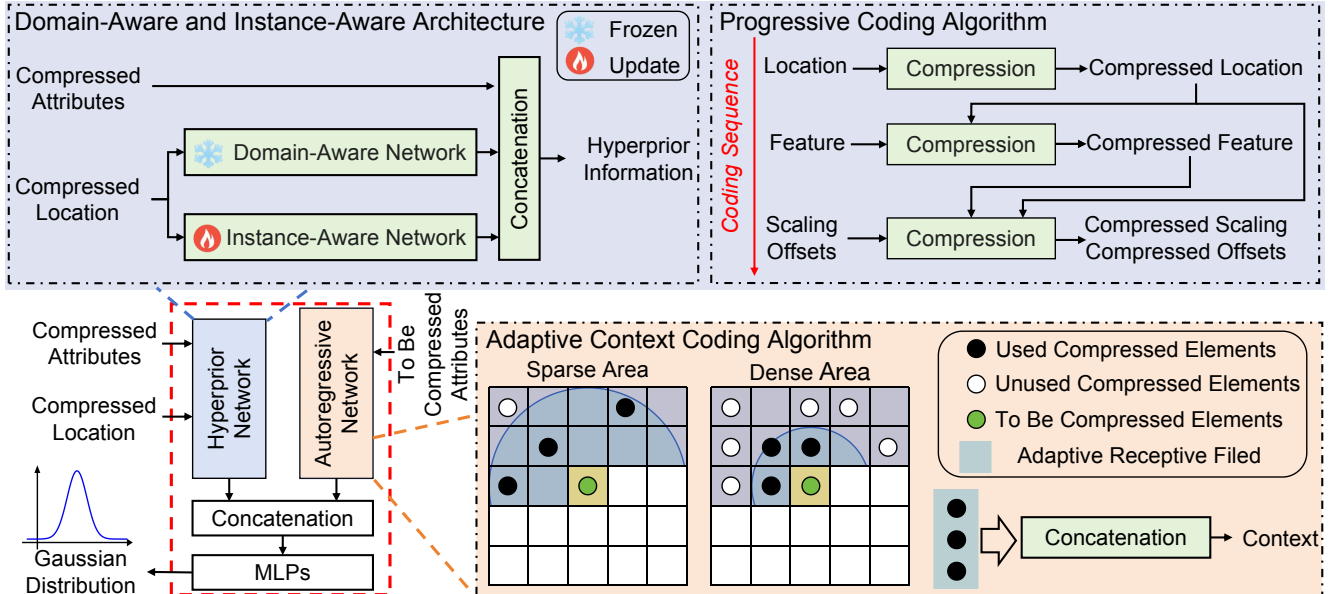


Figure 1. The details of our hybrid entropy model for Gaussian Splatting (HEMGS) data compression, which comprises a hyperprior network and an autoregressive network. The hyperprior network employs a progressive coding algorithm and incorporates domain-aware and instance-aware architectures to reduce redundancies across attributes. Furthermore, the autoregressive network utilizes an adaptive context coding algorithm with flexible receptive fields to reduce redundancies within each attribute.

scaling, and offsets. Compressing the anchors requires encoding both the location information and these attributes. In this work, we present a progressive coding algorithm that sequentially compresses anchor locations and those attributes. This algorithm uses previously compressed locations and attributes as prior information to aid in compressing subsequent attributes, effectively reducing structural redundancies across attributes. As shown in the top right-hand side of Fig. 2, the algorithm begins by quantizing anchor locations to 16-bit precision, as a common practice in most 3DGS compression methods [3, 20, 32, 36]. The quantized locations are then used as prior information to compress the local features. Subsequently, the quantized locations and compressed local features serve as prior features to further entropy code the scaling and offset attributes.

**Domain-Aware and Instance-Aware Network.** The progressive coding algorithm allows us to extract the information from the compressed locations and attributes for producing hyperprior information. However, how to effectively extract geometric information from anchor locations is a non-trivial process. Different from most existing methods primarily storing structural relationships in instance-aware MLPs [3, 26, 36], our approach employs both a domain-aware network and an instance-aware network to extract features from these compressed locations. Specifically, as illustrated in the top left-hand side of Figure 2, our domain-aware network leverages the capabilities of a pre-trained 3D feature extractor, such as PointNet++ [33], to effectively capture domain-aware structural

relationships while introducing no additional storage overhead. Meanwhile, we directly employ a hash-grid assisted context method as in [3] to encode the structural relationships of individual scene-specific instances. By combining both domain-aware and instance-aware structural relationships, we produce a comprehensive hyperprior, which enables more accurate distribution estimation for anchor attributes, enhancing the efficiency of conditional entropy coding for local features.

Combined with our progressive coding algorithm, we first employ the domain-aware and instance-aware network to extract location information for compressing local feature attributes. Then, when compressing scaling and offset attributes, we integrate the compressed local feature attributes and utilize the location features produced by the domain-aware and instance-aware network once again. This dual-path network generates a more refined hyperprior feature for effectively coding the local feature, scaling and offset attributes.

Overall, the efficient hyperpriors obtained through the hyperprior network enable accurate estimation of anchor attribute distributions, reducing redundancy across attributes and improving compression performance.

### 3.2.2. Autoregressive Network

Inspired by classic autoregressive coding mechanisms in NIC and NVC methods [8, 13, 21, 28, 34, 35], which effectively reduce redundancy, we have designed an autoregressive network specifically for 3D Gaussian Splatting (3DGS) to address structural redundancies within its attributes. This

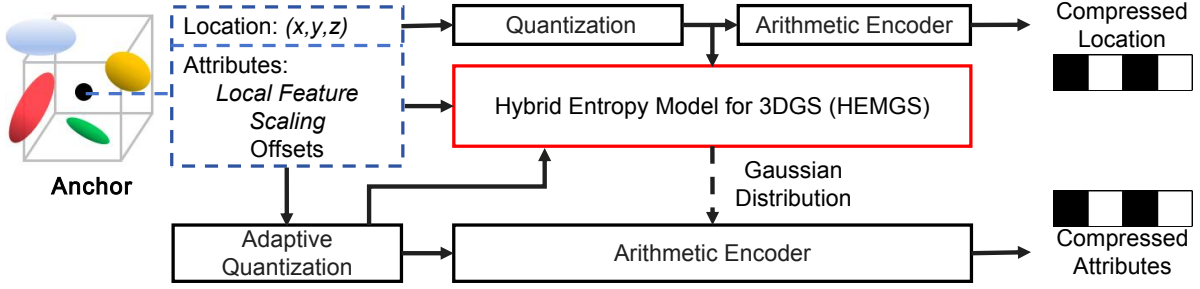


Figure 2. The overview of our 3DGS data compression framework, which integrates HEMGS with additional other coding components.

network employs a newly proposed adaptive context coding algorithm to eliminate redundancy within each attribute, as illustrated in the bottom side of Figure 1.

Given that those anchor-based methods [3, 26, 36] partition the 3D scene into voxels and treat the center of each non-empty voxel as an anchor point, we compress the anchors within the voxels in raster order. During the compression of an attribute, elements within the attribute can use surrounding already-encoded elements as contextual information. This approach reduces redundancy between adjacent elements and improves 3DGS data compression performance.

**Adaptive Context Coding Algorithm.** Additionally, due to the varying density of anchors across different regions, we introduced an adaptive context coding algorithm to optimize the extraction of contextual information, as shown in Figure 1. In sparse areas, we enlarge the receptive field to gather more elements as contextual information, ensuring that even isolated anchors have sufficient context for accurate encoding. While, in dense areas, we reduce the receptive field and select only the  $n$  closest elements, focusing on providing highly relevant contextual information and ensuring that the most significant features are prioritized in regions with high density.

### 3.3. Overall Framework with HEMGS

We seamlessly integrate our HEMGS with additional coding components, including the quantization, the adaptive quantization, and the arithmetic encoder into a 3DGS compression network, as shown in Figure 2.

Our goal is to compress both location and attributes. We first compress location information by quantizing it to 16-bit precision. Then, we adopt the adaptive quantization strategy as in HAC [3] for quantizing the attributes, which generates an adaptive quantization scale  $Q$  leveraging the compressed location information. Subsequently, our HEMGS models the Gaussian distribution for entropy encoding the quantized attributes, leveraging the anchor location as prior information. An arithmetic encoder module is then applied to losslessly convert these quantized attributes into a bit-stream (*i.e.*, storage), ensuring a compact and efficient representation.

Each anchor is defined by a location  $x^a$  and a set of at-

tributes  $\mathcal{A} = \{f^a, l, o\}$ . For the quantized  $i$ -th attribute vector  $\hat{\mathcal{A}}_i$ , the probability of  $\hat{\mathcal{A}}_i$  can be estimated as,

$$p_{\hat{\mathcal{A}}_i}(\hat{\mathcal{A}}_i | \hat{x}^a, \hat{\mathcal{A}}_{<i}, \theta_{hp}, \theta_{ar}, \theta_{mlp}) = \prod_j \left( \mathcal{N}(\mu_{i,j}, \sigma_{i,j}^2) * \mathcal{U}\left(-\frac{1}{2} * Q_{i,j}, \frac{1}{2} * Q_{i,j}\right) \right) (\hat{\mathcal{A}}_{i,j})$$

with  $\mu_{i,j}, \sigma_{i,j} = g_{mlp}(\psi_{i,j}, \phi_{i,j}; \theta_{mlp})$ ,  
 $\psi_{i,j} = g_{hp}(\hat{x}^a, \hat{\mathcal{A}}_{<i}; \theta_{hp})$ ,  
 $\phi_{i,j} = g_{ar}(\hat{\mathcal{A}}_{i,<j}; \theta_{ar})$ .

(2)

where  $j$  specifies the index of the attribute element.  $\psi$ ,  $\phi$  is the output of our hyperprior network and autoregressive network, respectively. Note that after obtaining  $\psi$  and  $\phi$ , HEMGS utilizes MLPs, which is denoted as  $g_{mlp}$ , to generate  $\mu$  and  $\sigma$  for Gaussian distribution. According to the progressive coding algorithm in our hyperprior network, the previously compressed attribute is denoted as  $\hat{\mathcal{A}}_{<i}$ .  $\theta_{hp}, \theta_{ar}, \theta_{mlp}$  are the learned parameters of our hyperprior network, autoregressive network, and the MLPs in our HEMGS.  $\mu_{i,j}, \sigma_{i,j}$  are the mean and variance of the  $j$ -th element in  $i$ -th attribute.  $Q_{i,j}$  is the quantization scale of the  $j$ -th element belonging to the  $i$ -th attribute.  $g_{hp}$ , and  $g_{ar}$  are our hyperprior network, and autoregressive network in HEMGS. In our autoregressive network, the context of  $\hat{\mathcal{A}}_{i,j}$  is denoted as  $\hat{\mathcal{A}}_{i,<j}$ .

**Optimization Strategy.** The entire 3DGS data compression network can be optimized as below,

$$\mathcal{L} = \mathcal{L}_{\text{Rendering}} + \lambda \mathcal{L}_{\text{anchor}} \quad (3)$$

The term  $\mathcal{L}_{\text{Rendering}}$  is the rendering loss as specified in [26]. The term  $\mathcal{L}_{\text{anchor}}$  denotes the estimated storage consumption for anchor, which is primarily consumed by the compressed attributes as mentioned previously, along with some auxiliary items used in the classical anchor-based 3DGS data compression framework [3]. The hyperparameters  $\lambda$  serve to balance these two loss components.

## 4. Experiment

### 4.1. Datasets

We conducted comprehensive experiments on multiple datasets, including the small-scale Synthetic-

Table 1. Comparison of the newly proposed HEMGS method with other 3DGS data compression methods, including 3DGS and Scaffold-GS, for reference. For our approach, we report two sets of results by considering different trade-offs between size and fidelity, which are achieved by adjusting the parameter  $\lambda$ . The best and second-best results are highlighted in red and yellow cells, respectively. The size values are measured in megabytes (MB).

Datasets	Mip-NeRF360 [2]				Tank&Temples [19]				DeepBlending [14]				Synthetic-NeRF [27]			
Methods	psnr $\uparrow$	ssim $\uparrow$	lpips $\downarrow$	size $\downarrow$	psnr $\uparrow$	ssim $\uparrow$	lpips $\downarrow$	size $\downarrow$	psnr $\uparrow$	ssim $\uparrow$	lpips $\downarrow$	size $\downarrow$	psnr $\uparrow$	ssim $\uparrow$	lpips $\downarrow$	size $\downarrow$
3DGS [17]	27.49	0.813	0.222	744.7	23.69	0.844	0.178	431.0	29.42	0.899	0.247	663.9	33.80	0.970	0.031	68.46
Scaffold-GS [26]	27.50	0.806	0.252	253.9	23.96	0.853	0.177	86.50	30.21	0.906	0.254	66.00	33.41	0.966	0.035	19.36
EAGLES [10]	27.15	0.808	0.238	68.89	23.41	0.840	0.200	34.00	29.91	0.910	0.250	62.00	32.54	0.965	0.039	5.74
LightGaussian [9]	27.00	0.799	0.249	44.54	22.83	0.822	0.242	22.43	27.01	0.872	0.308	33.94	32.73	0.965	0.037	7.84
Compact3DGS [20]	27.08	0.798	0.247	48.80	23.32	0.831	0.201	39.43	29.79	0.901	0.258	43.21	33.33	0.968	0.034	5.54
Compressed3D [30]	26.98	0.801	0.238	28.80	23.32	0.832	0.194	17.28	29.38	0.898	0.253	25.30	32.94	0.967	0.033	3.68
Morgen. <i>et al.</i> [29]	26.01	0.772	0.259	23.90	22.78	0.817	0.211	13.05	28.92	0.891	0.276	8.40	31.05	0.955	0.047	2.20
Navaneet <i>et al.</i> [30]	27.16	0.808	0.228	50.30	23.47	0.840	0.188	27.97	29.75	0.903	0.247	42.77	33.09	0.967	0.036	4.42
HAC [3]	27.77	0.811	0.230	21.87	24.40	0.853	0.177	11.24	30.34	0.906	0.258	6.35	33.71	0.968	0.034	1.86
Context-GS [36]	27.72	0.811	0.231	21.58	24.29	0.855	0.176	11.80	30.39	0.909	0.258	6.60	-	-	-	-
Ours (low-rate)	27.74	0.807	0.249	11.96	24.40	0.848	0.192	5.75	30.24	0.909	0.270	2.85	33.56	0.967	0.037	1.20
Ours (high-rate)	27.94	0.813	0.230	20.03	24.55	0.856	0.176	9.67	30.40	0.912	0.258	6.39	33.82	0.968	0.034	1.62

NeRF dataset [27] and three large-scale real-scene datasets: DeepBlending [14], Mip-NeRF360 [2], and Tanks&Temples [19].

## 4.2. Experiment Details

**Benchmarks.** We compare our HEMGS with existing 3DGS data compression methods. Some methods [9, 20, 30, 31] primarily achieve compact representations of 3DGS through parameter pruning or codebook-based strategies. Other methods [3, 26, 29, 36] exploit the structural relationships within 3DGS for compression. Notably, HAC [3] and Context-GS [36] have achieved impressive results in 3DGS compression by utilizing instance-aware hash-grids and anchor-level context to capture structural redundancies, respectively.

**Evaluation Metric.** We measure the storage used for compressed 3DGS data using the metric of storage size in megabytes (MB). The quality of the rendered images from the compressed 3DGS data is evaluated using the Peak Signal-to-Noise Ratio (PSNR), Structural Similarity Index (SSIM) [37], and Learned Perceptual Image Patch Similarity (LPIPS) [39] metrics.

**Implementation Details.** Our HEMGS is implemented in PyTorch with CUDA support. All experiments are conducted on a machine with an NVIDIA A800 GPU (80GB memory). We use the Adam optimizer [18] and train our HEMGS for 60,000 iterations. Following HAC [3], we adjust  $\lambda$  from  $5e - 4$  to  $4e - 3$  in order to balance the rate-distortion tradeoffs. In our autoregressive network, we set a large receptive field of  $25 \times 25 \times 25$  at the voxel level and select the 20 closest elements within this field. The MLPs in our HEMGS consist of a single 2-layer MLP with ReLU activation.

## 4.3. Experiment Results

The compression results are presented in Table 1. Our HEMGS achieves a substantial size reduction of over 100x compared to the 3DGS [17], while maintaining improved fidelity. Additionally, it reduces size by over 18x on average when compared to Scaffold-GS [26]. Furthermore, the proposed method demonstrates superior storage efficiency compared to recent state-of-the-art 3DGS data compression methods, such as HAC [3] and Context-GS [36]. The RD curves for different compression methods are provided in Figure 3. Compared to our baseline method, HAC [3], our approach consistently achieves higher PSNR across all storage levels. Specifically, our HEMGS saves 44.68% storage at 27.8 PSNR on the Mip-NeRF360 dataset [2] and 48.21% storage at 24.4 PSNR on the Tank&Temples dataset [19] compared to HAC. Overall, our approach achieves an average storage savings of approximately 40% across all benchmark datasets, including Mip-NeRF360 [2], Tank&Temples [19], DeepBlending [14], and Synthetic-NeRF [27]. We also report the BDBR [11] results in Table 2, showing that HAC and Context-GS require 71.17% and 56.14% more storage, respectively, than our newly proposed HEMGS at the same PSNR on the Mip-NeRF360 dataset. This demonstrates that our method outperforms the recent state-of-the-art approach, HAC, and highlights the efficiency of our newly proposed HEMGS for 3DGS data compression.

## 4.4. Ablation Study

In this subsection, we conduct ablation studies to evaluate the effectiveness of each technical component. Experiments are performed on the “playroom” scene in the DeepBlending dataset [14], as shown in Table 3. To demonstrate the

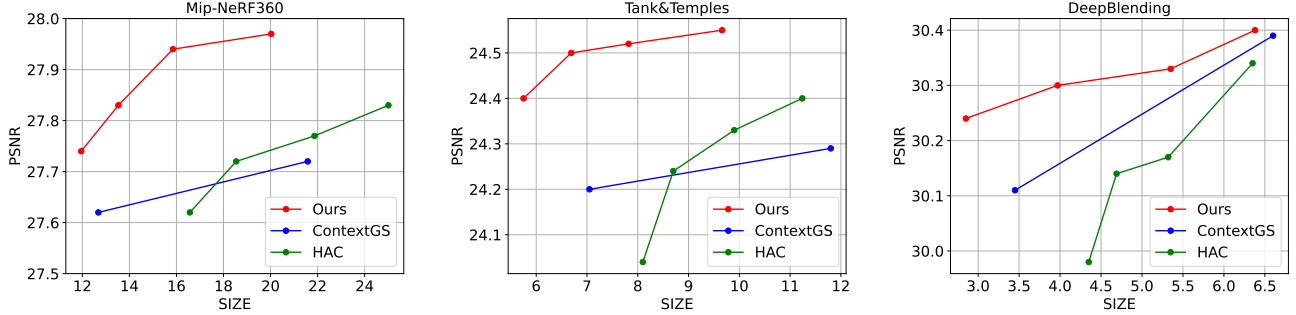


Figure 3. The Rate-Distortion (RD) curves on three benchmark datasets, including Mip-NeRF360, Tank&Temples, and DeepBlending.

Table 2. BDBR (%) results for HAC, Context-GS, and our newly proposed HEMGS across different datasets. Positive BDBR values indicate additional storage costs than our HEMGS.

	Mip-NeRF360	DeepBlending
Context-GS [36]	56.14	21.99
HAC [3]	71.17	86.66

Table 3. Ablation study of each newly proposed component, which is measured on the “playroom” scene in the DeepBlending dataset with  $\lambda = 2e - 3$ . “PC”, “DA”, and “AR” denote the Progressive Coding algorithm, Domain-Aware network, and AutoRegressive network, respectively.

Methods	PSNR $\uparrow$	Size (MB) $\downarrow$
Ours	30.96	3.12
Ours w/o PC	30.82	3.37
Ours w/o PC and DA	30.69	3.55
Ours w/o PC, DA, and AR	30.66	4.12

impact of the progressive coding algorithm, we remove it from our method (denoted as “Our w/o PC”), resulting in a 0.45% PSNR decrease and an additional 7.42% storage cost. To assess the Domain-Aware network, we remove it from “Ours w/o PC” (denoted as “Ours w/o PC and DA”), leading to a 0.42% PSNR decrease and an additional 5.07% storage cost. For the autoregressive network, we further remove it from “Ours w/o PC and DA” (denoted as “Ours w/o PC, DA, and AR”), resulting in a 0.1% PSNR decrease and an additional 4.12% storage cost. These results demonstrate the effectiveness of our progressive coding algorithm, Domain-Aware network, and autoregressive network in enhancing PSNR while reducing storage requirements.

To measure the impact of our adaptive context coding algorithm and large receptive field in our autoregressive network, we conduct an ablation study, as shown in Table 4. To evaluate the effectiveness of our adaptive context coding algorithm, we remove this component from our method, namely “Ours\* w/o ACC”. The results for “Ours\* w/o ACC” show an additional 0.2 MB storage cost compared to our method (“Ours\*”). To assess the impact of a large receptive field ( $25 \times 25 \times 25$ ), we reduce it to  $5 \times 5 \times 5$  as in NIC methods, resulting in “Ours\* with SRF”. Notably, the small receptive field captures an average of only 0.43 an-

Table 4. Ablation study of the adaptive context coding algorithm and large receptive field, two components of the autoregressive network, on the “playroom” scene in the DeepBlending dataset with  $\lambda = 2e - 3$ . The average and maximum anchor numbers in the receptive field along with the performance of the compressed 3D scene are reported. “ACC”, and “SRF” represent the Adaptive Context Coding algorithm, and Small Receptive Filed ( $5 \times 5 \times 5$ ) as in NIC methods, respectively. “Ours\*” refers to our method without the domain-aware network and the progressive coding algorithm.

Methods	Anchor Number		Performance	
	Average	Max	PSNR $\uparrow$	Size $\downarrow$
Ours*	5.76	20	30.69	3.55
Ours* w/o ACC	6.15	80	30.69	3.75
Ours* with SRF	0.43	30	30.67	4.01

chor points, significantly fewer than the 5.76 anchor points obtained by our method. This change in “Ours\* with SRF” incurs an additional 0.26 MB storage cost and a 0.02 dB PSNR drop compared to “Ours\* w/o ACC”. These results demonstrate the effectiveness of our adaptive context coding algorithm and large receptive field.

To further evaluate the effectiveness of our HEMGS, we compared the storage requirements for anchor locations and various attributes, as shown in Table 5. Our method reduces the storage needed for locations. For example, our approach achieves a 37% reduction in location storage compared to HAC [3] when  $\lambda = 4e - 3$ , demonstrating more efficient location compression. Additionally, our method decreases storage for anchor local features, achieving a 16.5% reduction compared to HAC at  $\lambda = 4e - 3$ . This improvement is due to the use of both domain-aware and instance-aware architectures to extract location features, combined with contextual information from the autoregressive model to predict local feature distributions, enabling efficient encoding. Furthermore, our method yields significant storage reductions for scaling and offset attributes. With  $\lambda = 4e - 3$ , storage is reduced by 40% and 58% for scaling and offset, respectively, compared to HAC. The greater reduction in scaling and offset is primarily due to using compressed features as prior information to predict the distribution of these at-

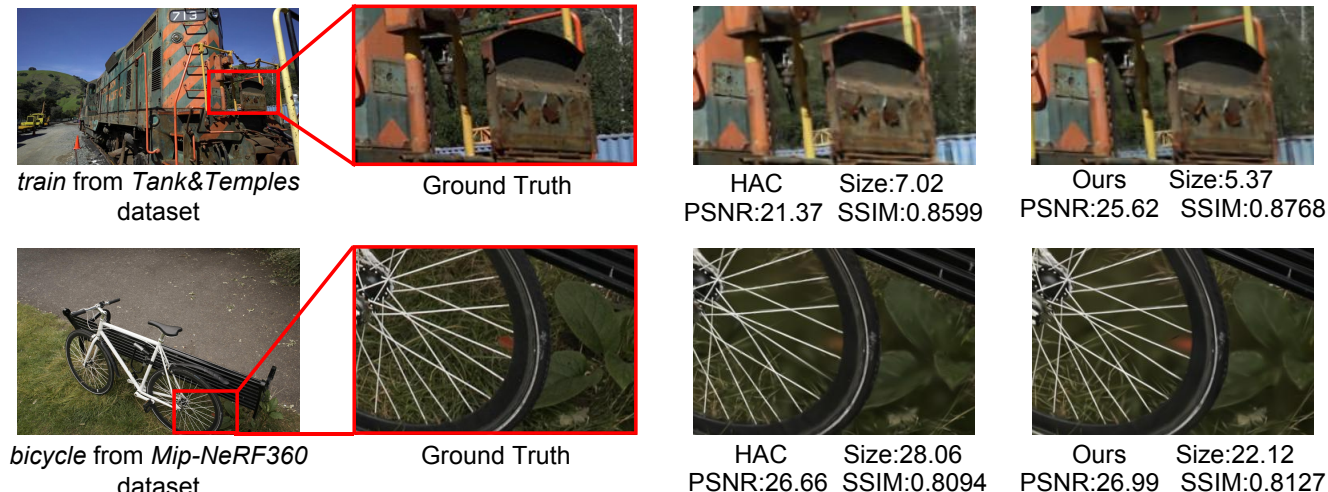


Figure 4. Visualization comparison between HAC and our newly proposed HEMGS on the “train” scene from the Tank&Temples dataset and the “bicycle” scene from the Mip-NeRF360 dataset. PSNR, SSIM of the rendered image and the size (MB) of the scene are reported.

Table 5. The storage cost of each component and the rendering qualities of HAC and our newly proposed HEMGS on the DeepBlending dataset. For a comprehensive comparison, we set  $\lambda$  to  $4e-3$  and  $5e-4$ . “Others” refers to additional storage costs (e.g., the parameters of MLPs).

Methods	Storage Cost (MB)↓						Fidelity↑	
	Location	Feature	Scaling	Offsets	Others	Total	PSNR	SSIM
HAC ( $\lambda = 4e-3$ )	0.897	1.366	0.716	0.974	0.362	4.318	30.22	0.908
Ours ( $\lambda = 4e-3$ )	0.567	1.140	0.428	0.411	0.308	2.854	30.24	0.909
HAC ( $\lambda = 5e-4$ )	0.983	3.519	1.218	1.590	0.391	7.501	30.36	0.911
Ours ( $\lambda = 5e-4$ )	0.815	3.407	0.800	0.988	0.378	6.387	30.40	0.912

tributes, effectively reducing structural redundancies. This further validates the effectiveness of our progressive coding algorithm in reducing attribute redundancy. Overall, compared to the baseline method HAC [3], our approach not only reduces storage consumption across most components but also achieves higher image fidelity, confirming the efficiency of our method.

#### 4.5. Visualization

Our visualization results are displayed in Figure 4, showing rendered outputs for the “train” scene from the Tank&Temples dataset [19] and the “bicycle” scene from the Mip-NeRF360 dataset [2]. Both our HEMGS and HAC [3] are trained with  $\lambda = 4e-3$  for fair comparison. In the “train” scene, our method produces sharper and more detailed renderings, particularly noticeable in the iron sheet at the front of the train. This enhanced detail is corroborated by improved fidelity metrics, such as PSNR and SSIM, demonstrating the superior quality of our method. Notably, despite achieving higher image fidelity, our approach requires less storage than HAC. In the “bicycle” scene, images rendered by our method display more distinct details, especially in the central region of the image, compared to HAC. Metrics including file size, PSNR, and SSIM consistently show that our approach preserves greater

image fidelity with reduced storage requirements. These visual comparisons effectively highlight the efficiency of our HEMGS approach.

## 5. Conclusion

In this work, we propose a HEMGS, which combines a hyperprior network and an autoregressive network to respectively reduce structural redundancies across and within attributes in 3DGS data. Integrated with other coding components, HEMGS achieves efficient 3DGS data compression and state-of-the-art performance across various 3DGS data compression benchmarks. The ablation study further validates the effectiveness of each component in HEMGS. This work will serve as a bridge for exploring effective entropy models tailored to the 3DGS data structure, paving the way for further advancements in the efficient compression and representation of this unique and complex data structure.

**Limitations and Future Works.** Currently, our method HEMGS applies only anchor-based 3DGS methods, which require the anchor structure to distribute local 3D Gaussians. In future work, we plan to extend our approach to anchor-free data structures, broadening its applicability.

## References

- [1] Johannes Ballé, David Minnen, Saurabh Singh, Sung Jin Hwang, and Nick Johnston. Variational image compression with a scale hyperprior. *Int. Conf. Learn. Represent.*, 2018. [1](#), [2](#), [3](#)
- [2] Jonathan T Barron, Ben Mildenhall, Dor Verbin, Pratul P Srinivasan, and Peter Hedman. Mip-nerf 360: Unbounded anti-aliased neural radiance fields. In *IEEE Conf. Comput. Vis. Pattern Recog.*, pages 5470–5479, 2022. [2](#), [6](#), [8](#)
- [3] Yihang Chen, Qianyi Wu, Weiyao Lin, Mehrtash Harandi, and Jianfei Cai. Hac: Hash-grid assisted context for 3d gaussian splatting compression. In *Eur. Conf. Comput. Vis.*, pages 422–438. Springer, 2025. [1](#), [2](#), [3](#), [4](#), [5](#), [6](#), [7](#), [8](#)
- [4] Zhenghao Chen, Shuhang Gu, Guo Lu, and Dong Xu. Exploiting intra-slice and inter-slice redundancy for learning-based lossless volumetric image compression. *IEEE Trans. Image Process.*, 31:1697–1707, 2022. [3](#)
- [5] Zhenghao Chen, Guo Lu, Zhihao Hu, Shan Liu, Wei Jiang, and Dong Xu. Lsvc: A learning-based stereo video compression framework. In *IEEE Conf. Comput. Vis. Pattern Recog.*, pages 6073–6082, 2022.
- [6] Zhenghao Chen, Lucas Relic, Roberto Azevedo, Yang Zhang, Markus Gross, Dong Xu, Luping Zhou, and Christopher Schroers. Neural video compression with spatio-temporal cross-covariance transformers. In *ACM Int. Conf. Multimedia*, pages 8543–8551, 2023.
- [7] Zhenghao Chen, Luping Zhou, Zhihao Hu, and Dong Xu. Group-aware parameter-efficient updating for content-adaptive neural video compression. *ACM Int. Conf. Multimedia*, pages 11022–11031, 2024.
- [8] Zhengxue Cheng, Heming Sun, Masaru Takeuchi, and Jiro Katto. Learned image compression with discretized gaussian mixture likelihoods and attention modules. In *Proceedings of the IEEE/CVF conference on computer vision and pattern recognition*, pages 7939–7948, 2020. [1](#), [2](#), [3](#), [4](#)
- [9] Zhiwen Fan, Kevin Wang, Kairun Wen, Zehao Zhu, De-jia Xu, and Zhangyang Wang. Lightgaussian: Unbounded 3d gaussian compression with 15x reduction and 200+ fps. *arXiv preprint arXiv:2311.17245*, 2023. [1](#), [3](#), [6](#)
- [10] Sharath Girish, Kamal Gupta, and Abhinav Shrivastava. Eagles: Efficient accelerated 3d gaussians with lightweight encodings. *arXiv preprint arXiv:2312.04564*, 2023. [6](#)
- [11] Bjontegaard Gisle. Calculation of average psnr differences between rd curves. In *VCEG-M33*, page 7, 2001. [6](#)
- [12] Tao Han, Zhenghao Chen, Song Guo, Wanghan Xu, Lei Bai, et al. Cra5: Extreme compression of era5 for portable global climate and weather research via an efficient variational transformer. *arXiv preprint arXiv:2405.03376*, 2024. [3](#)
- [13] Dailan He, Yaoyan Zheng, Baocheng Sun, Yan Wang, and Hongwei Qin. Checkerboard context model for efficient learned image compression. In *IEEE Conf. Comput. Vis. Pattern Recog.*, pages 14771–14780, 2021. [2](#), [3](#), [4](#)
- [14] Peter Hedman, Julien Philip, True Price, Jan-Michael Frahm, George Drettakis, and Gabriel Brostow. Deep blending for free-viewpoint image-based rendering. *ACM Trans. Graph.*, 37(6):1–15, 2018. [2](#), [6](#)
- [15] Zhihao Hu, Zhenghao Chen, Dong Xu, Guo Lu, Wanli Ouyang, and Shuhang Gu. Improving deep video compression by resolution-adaptive flow coding. In *Eur. Conf. Comput. Vis.*, pages 193–209. Springer, 2020. [3](#)
- [16] Zhihao Hu, Guo Lu, and Dong Xu. Fvc: A new framework towards deep video compression in feature space. In *IEEE Conf. Comput. Vis. Pattern Recog.*, pages 1502–1511, 2021. [1](#), [2](#), [3](#)
- [17] Bernhard Kerbl, Georgios Kopanas, Thomas Leimkühler, and George Drettakis. 3d gaussian splatting for real-time radiance field rendering. *ACM Trans. Graph.*, 42(4):139–1, 2023. [1](#), [3](#), [6](#)
- [18] Diederik P Kingma. Adam: A method for stochastic optimization. *Int. Conf. Learn. Represent.*, 2015. [6](#)
- [19] Arno Knapitsch, Jaesik Park, Qian-Yi Zhou, and Vladlen Koltun. Tanks and temples: Benchmarking large-scale scene reconstruction. *ACM Trans. Graph.*, 36(4):1–13, 2017. [2](#), [6](#), [8](#)
- [20] Joo Chan Lee, Daniel Rho, Xiangyu Sun, Jong Hwan Ko, and Eunbyung Park. Compact 3d gaussian representation for radiance field. In *IEEE Conf. Comput. Vis. Pattern Recog.*, pages 21719–21728, 2024. [1](#), [3](#), [4](#), [6](#)
- [21] Jiahao Li, Bin Li, and Yan Lu. Deep contextual video compression. *Advances in Neural Information Processing Systems*, 34, 2021. [1](#), [2](#), [3](#), [4](#)
- [22] Lei Liu, Zhihao Hu, Zhenghao Chen, and Dong Xu. Icmhnet: Neural image compression towards both machine vision and human vision. In *ACM Int. Conf. Multimedia*, pages 8047–8056, 2023.
- [23] Lei Liu, Zhihao Hu, and Jing Zhang. Pchm-net: A new point cloud compression framework for both human vision and machine vision. *Int. Conf. Multimedia and Expo*, 2023.
- [24] Lei Liu, Zhihao Hu, and Zhenghao Chen. Towards point cloud compression for machine perception: A simple and strong baseline by learning the octree depth level predictor. In *Generalizing from Limited Resources in the Open World*, pages 3–17, Singapore, 2024. Springer Nature Singapore.
- [25] Guo Lu, Wanli Ouyang, Dong Xu, Xiaoyun Zhang, Chunlei Cai, and Zhiyong Gao. Dvc: An end-to-end deep video compression framework. In *IEEE Conf. Comput. Vis. Pattern Recog.*, pages 11006–11015, 2019. [1](#), [2](#), [3](#)
- [26] Tao Lu, Mulin Yu, Linning Xu, Yuanbo Xiangli, Limin Wang, Dahua Lin, and Bo Dai. Scaffold-gs: Structured 3d gaussians for view-adaptive rendering. In *IEEE Conf. Comput. Vis. Pattern Recog.*, pages 20654–20664, 2024. [1](#), [2](#), [3](#), [4](#), [5](#), [6](#)
- [27] Ben Mildenhall, Pratul P Srinivasan, Matthew Tancik, Jonathan T Barron, Ravi Ramamoorthi, and Ren Ng. Nerf: Representing scenes as neural radiance fields for view synthesis. *Communications of the ACM*, 65(1):99–106, 2021. [1](#), [2](#), [6](#)
- [28] David Minnen, Johannes Ballé, and George D Toderici. Joint autoregressive and hierarchical priors for learned image compression. *Adv. Neural Inform. Process. Syst.*, 31, 2018. [1](#), [2](#), [3](#), [4](#)
- [29] Wieland Morgenstern, Florian Barthel, Anna Hilsmann, and Peter Eisert. Compact 3d scene representation via self-

- organizing gaussian grids. *Eur. Conf. Comput. Vis.*, 2025. 1, 3, 6
- [30] KL Navaneet, Kossar Pourahmadi Meibodi, Soroush Abbasi Koohpayegani, and Hamed Pirsiavash. Compact3d: Compressing gaussian splat radiance field models with vector quantization. *arXiv preprint arXiv:2311.18159*, 2023. 1, 3, 6
- [31] Simon Niedermayr, Josef Stumpfegger, and Rüdiger Westermann. Compressed 3d gaussian splatting for accelerated novel view synthesis. In *IEEE Conf. Comput. Vis. Pattern Recog.*, pages 10349–10358, 2024. 1, 3, 6
- [32] Panagiotis Papantonakis, Georgios Kopanas, Bernhard Kerbl, Alexandre Lanvin, and George Drettakis. Reducing the memory footprint of 3d gaussian splatting. *Proceedings of the ACM on Computer Graphics and Interactive Techniques*, 7(1):1–17, 2024. 4
- [33] Charles Ruizhongtai Qi, Li Yi, Hao Su, and Leonidas J Guibas. Pointnet++: Deep hierarchical feature learning on point sets in a metric space. *Adv. Neural Inform. Process. Syst.*, 30, 2017. 2, 4
- [34] Yichen Qian, Zhiyu Tan, Xiuyu Sun, Ming Lin, Dongyang Li, Zhenhong Sun, Li Hao, and Rong Jin. Learning accurate entropy model with global reference for image compression. In *Int. Conf. Learn. Represent.*, 2021. 2, 3, 4
- [35] Yichen Qian, Xiuyu Sun, Ming Lin, Zhiyu Tan, and Rong Jin. Entroformer: A transformer-based entropy model for learned image compression. In *Int. Conf. Learn. Represent.*, 2022. 2, 3, 4
- [36] Yufei Wang, Zhihao Li, Lanqing Guo, Wenhan Yang, Alex C Kot, and Bihan Wen. Contextgs: Compact 3d gaussian splatting with anchor level context model. *arXiv preprint arXiv:2405.20721*, 2024. 3, 4, 5, 6, 7
- [37] Zhou Wang, Alan C Bovik, Hamid R Sheikh, and Eero P Simoncelli. Image quality assessment: from error visibility to structural similarity. *IEEE Trans. Image Process.*, 13(4): 600–612, 2004. 6
- [38] Qiang Zhang, Seung-Hwan Baek, Szymon Rusinkiewicz, and Felix Heide. Differentiable point-based radiance fields for efficient view synthesis. In *SIGGRAPH Asia 2022 Conference Papers*, pages 1–12, 2022. 3
- [39] Richard Zhang, Phillip Isola, Alexei A Efros, Eli Shechtman, and Oliver Wang. The unreasonable effectiveness of deep features as a perceptual metric. In *IEEE Conf. Comput. Vis. Pattern Recog.*, pages 586–595, 2018. 6